JOURNAL OF MATERIALS SCIENCE **37** (2002) 1315 – 1320

Lithiation reactions of Zn- and Li-birnessites in non-aqueous solutions and their stabilities

LIHUI LIU
Fracture Research Institute, Tohoku University, Aza-Aoba 01, Aramaki, Aoba-ku, Sendai 980-8579, Japan

QI FENG[*,‡], K. YANAGISAWA
Research Laboratory of Hydrothermal Chemistry, Faculty of Science, Kochi University, Akebono-cho, 2-5-1, Kochi-shi, 780-8520, Japan

G. BIGNALL
Department of Geoscience and Technology, Tohoku University, Aza-Aoba 01, Aramaki, Aoba-ku, Sendai 980-8579, Japan

T. HASHIDA
Fracture Research Institute, Tohoku University, Aza-Aoba 01, Aramaki, Aoba-ku, Sendai 980-8579, Japan

Zn- and Li-birnessites were synthesized from Na-birnessite by ion-exchange reactions. The ion-exchange reaction, chemical lithiation reaction in non-aqueous solution, and stability for these birnessites were investigated by XRD, TG-DTA, and chemical analyses. The Zn-birnessite showed greater thermal stability than Li-birnessite. The Zn- and Li-birnessites can be lithiated up to Li/Mn molar ratios of 0.45 and 1.08, respectively, by reaction in a LiI-acetonitrile solution. The lithiation of Zn-birnessite progressed by a redox topotactic reaction, but the Li-birnessite was unstable during the lithiation reaction. The lithiated Zn-birnessite showed greater thermal stability than lithiated Li-birnessite. The Zn species in the interlayer space of lithiated Zn-birnessite acts as a pillar for the stabilization of the layered structure. © *2002 Kluwer Academic Publishers*

1. Introduction

Recently, rechargeable lithium batteries have become widely used in mobile devices, such as cellular phones and portable computers. Commercial rechargeable lithium batteries consist of two intercalation compounds, with $LiCoO_2$ as the positive electrode and graphite as the negative electrode. Despite the successful application of $LiCoO_2$, development of the next generation of rechargeable lithium batteries is critically dependent on replacing this positive electrode material. The goal is a low cost synthesis of new lithium transition metal oxides, which fulfill the requirements of positive electrode materials, with a lower toxicity and a higher capacity on the charge-discharge cycling than $LiCoO_2$ (which has a capacity about 130 mAh/g) [1].

Much attention has focused on lithium manganese oxides, due to their low cost and toxicity [2, 3]. $LiMn_2O_4$ spinel has been investigated, but it only stores 120 mAh/g of charge, and capacity decreases rapidly during the charge-discharge cycling [1]. $LiMnO_2$ layered compounds appear more suitable, since most of the lithium can be removed and reinserted during the cycling process, and they have a theoretical capacity of 285 mAh/g [1]. However, the capacity of $LiMnO_2$ layered compounds decreases during the discharge-charge process, since the layered structure is transformed to a spinel structure [4–7].

Na-birnessite is a layered manganese oxide with a structure of stacking edge-shared MnO_6 octahedral layers with crystal water molecules and Na^+ ions between the MnO_6 octahedral layers [8]. Na^+ can be exchanged with other metal ions by ion-exchange reactions [9]. Birnessite-type manganese oxides have been investigated as cathodic material in lithium rechargeable batteries [10–12]. It has been found that the birnessites have high initial capacities, up to 200 mAh/g, although capacities decrease rapidly during the charge-discharge cycling. Na- and K-birnessites give better cycling performance than other birnessites, because Na^+ and K^+ ions act as pillars to stabilize the layered structure of the birnessite [13, 14]. Only a few studies have focused on the lithium intercalation reaction with M^{2+}-birnessites (M^{2+} = divalent metal ion) [15]. Goff *et al.* studied the electrochemical properties of several birnessites, and found that Zn-birnessite exhibited the greatest capacity [16]. Even so, specifics of the lithium intercalation

---

[*] Author to whom all correspondence should be addressed.

[‡] *Present Address*: Faculty of Engineering, Kagawa University, Hayashi-cho, 2217-20, Takamatsu-shi, 761-0396, Japan.

reaction in birnessite remains unclear, and the thermal stabilities of Li-intercalated birnessites require further investigation.

We have studied the synthesis of Na-birnessite and its electrochemical properties [17, 18]. The Na-birnessite showed an initial capacity of 200 mAh/g, and the capacity degraded to 150 mAh/g after 5 cycles in the working potential range of 2.0 to 4.0 V. Herein, we describe the synthesis of Zn- and Li-birnessite from Na-birnessite by ion-exchange reaction, the chemical lithiation of birnessite in non-aqueous solutions, and the characterization of birnessite by powder XRD, thermogravimetric analysis (TG-DTA), and chemical analysis.

2. Experiment

Na-birnessite (Na-B) was prepared by hydrothermal treatment of a low crystalline Na-birnessite in a 2 M NaOH solution at 175°C for 24 hr as described previously [17]. The low crystalline was obtained by pouring a mixed solution comprises (100 mL) 0.6 M NaOH and 3% H_2O_2 into a (50 mL) 0.3 M $Mn(NO_3)_2$ solution, while stirring vigorously at room temperature, and then aging in the reaction solution for 24 h. Zn-birnessite (Zn-B) was synthesized from a Na-B (10 g) sample by ion-exchange treatment in a 2 M $ZnCl_2$ solution (1 L). The ion-exchange treatment was repeated for two times to complete the reaction. The Na-B (10 g) was initially treated with a 1 M HNO_3 solution (1 L) at room temperature to prepare H-birnessite. Li-birnessite (Li-B) was obtained by ion-exchange treatment of the H-birnessite (10 g) in a 2 M LiOH solution (1 L). Samples of Zn-B and Li-B were heated at a desired temperature for 4 hr to investigate their thermal stabilities. Heat-treated Zn-B (1 g) and Li-B (1 g) were lithiated in LiI-acetonitrile solutions (15 mL).

The chemical compositions of the samples were determined by atomic absorption spectrometry (HITACHI 180-60) after dissolution in a mixed solution of H_2O_2 and HCl. The mean oxidation number (Z_{Mn}) of manganese was determined by the standard oxalic acid method as described previously [19]. X-ray diffraction (XRD) analysis was undertaken using an X-ray diffractometer (Rigaku, RTP300RC) with Cu K_α ($\lambda = 0.15418$ nm) radiation. Thermogravimetric analysis was performed on a thermal analyzer (Seiko, TG-DTA320) at a heating rate of 10°C/min.

3. Results and discussion

3.1. Synthesis of Na-, Zn-, and Li-birnessites

A hydrothermally prepared Na-birnessite (Na-B) with high crystallinity was used as a precursor for the synthesis of Zn-birnessite and Li-birnessite. Fig. 1a shows the XRD pattern of Na-B. The Na-B has a layered structure, formed by stacking two-dimensional sheets of edge-shared MnO_6 octahedra, with basal spacing of 0.723 nm, and crystal water and Na^+ occurring between the sheets of MnO_6 octahedra [8, 9]. Na^+ in the interlayer space are ion-exchangeable with other cations.

Fig. 1b shows the XRD pattern for Zn-birnessite (Zn-B) that was obtained by ion-exchange treatment of Na-B, using a 2 M $ZnCl_2$ solution. We used the concentrated $ZnCl_2$ solution, because $Zn(OH)_2$ precipitate easily forms in a diluted $ZnCl_2$ solution, such as a 0.5 M $ZnCl_2$ solution. The layered structure of the birnessite retained after the ion-exchange reaction, although the basal spacing shifts from 0.723 to 0.718 nm. The complete exchange of Na^+ in birnessite by Li^+ using a direct ion-exchange reaction of Na-B with lithium salt solution is not readily achieved, so a two-step ion-exchange process was used to synthesize a perfectly Li-exchanged birnessite [20]. Firstly, Na-B was treated with a HNO_3 solution to transform Na-B to a H-birnessite, and then the H-birnessite was reacted with a LiOH solution to exchange H^+ in the birnessite with Li^+. XRD results (Fig. 1c) indicate that the two-step ion-exchange reaction proceeds topotactically, and that the obtained Li-B has a layered structure with a basal spacing of 0.718 nm.

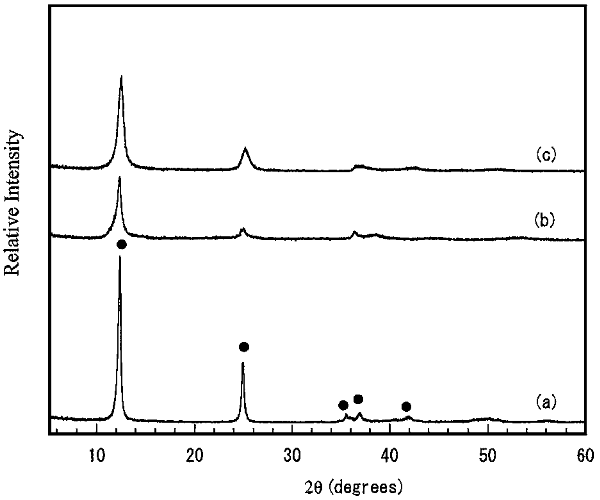

Figure 1 XRD patterns of (a) Na-B, (b) Zn-B and (c) Li-B. ●: Na-birnessite phase.

The chemical compositions of Na-B, Zn-B, and Li-B are summarized in Table I. The Li/Mn molar ratio in Li-B is little less than the Na/Mn molar ratio in the precursor Na-B, and the mean oxidation number (Z_{Mn}) of manganese in Li-B is higher than that in Na-B, suggesting that except the ion-exchange reaction, a redox reaction occurs also in the two-steps ion-exchange process [19]. When Na-B is treated in HNO_3 solution, a disproportionation reaction of Mn(III) to Mn(IV) and Mn(II) occurs, where Mn(II) dissolves in the solution phase and Mn(IV) remains in the solid phase. After the acid-treatment, all manganese ions in H-B are in tetravalent state. The Z_{Mn} value of Li-B obtained by treatment of H-B with LiOH solution is 4.0, suggesting that most

TABLE I Chemical compositions, and structural parameters of Na-birnessite used as precursor, and Zn- and Li-birnessites prepared by ion-exchange reactions

Sample	Basal spacing (nm)	Z_{Mn}	Composition (molar ratio)		
			Zn/Mn	Li/Mn	Na/Mn
Na-B	0.723	3.8	–	–	0.49
Zn-B	0.718	3.8	0.24	–	0.13
Li-B	0.718	4.0	–	0.47	–

Li^+ are inserted into the birnessite by a Li^+/H^+ ion-exchange reaction.

After ion-exchange treatment with $ZnCl_2$ solution, Na/Mn molar ratio in the Na-B decreased to 0.13, the Zn/Mn molar ratio increased to 0.24, and Z_{Mn} value did not changed (Table I), indicating that an ion-exchange reaction occurred, in which 73% of Na^+ in Na-B was exchanged. However, the ion-exchange was not a simple Zn^{2+}/Na^+ exchange reaction, because the Zn/Mn molar ratio (0.24) was higher than the Zn/Mn molar ratio (0.18) anticipated from the exchanged Na/Mn molar ratio (0.36). This fact suggests that some anions are also inserted into the birnessite during the ion-exchange treatment.

Recently, we have investigated the ion-exchange reaction of $Na^+/Ni^{2+}$and $Ni(OH)_2$ intercalation reaction for Na-birnessite [21]. Except the ion-exchange reaction, $NiOH^+$ and $Ni(OH)_2$ can be also inserted easily into the interlayer space of the birnessite in a neutral solution, and the hydroxides are preferentially formed in the interlayer space rather than in the solution phase. In the present case, when concentrated $ZnCl_2$ solution was diluted, such as to 0.5 M $ZnCl_2$ solution, $Zn(OH)_2$ precipitate was formed. This fact indicates that Zn^{2+} has a strong tendency in a neutral solutions to form $Zn(OH)_2$ and hydroxide complex ions, such as $Zn(OH)^+$. We believe some Na^+ is also exchanged with the hydroxide complex ions, as well as Zn^{2+} during the ion-exchange treatment. Blake *et al.* [15] have studied a Zn-birnessite prepared by ion-exchange treatment Na-birnessite with $Zn(NO_3)_2$ solution, and found that the birnessite contained CO_3^{2-} and NO_3^- ions. Although the insertion of CO_3^{2-} into the birnessite is also possible, but the amount of CO_3^{2-} will be much less than OH^-, due to the high negative charge of CO_3^{2-}. In fact, an IR study indicated that a small band at 1394 cm^{-1}, which corresponds to NO_3^-, was observed for Na-B sample. However, after the ion-exchange treatment with $ZnCl_2$ solution, this band disappeared, and no band corresponding to $CO_3^{2-}$was observed for Zn-B sample.

The chemical formula for Na-B can be written as $Na_{0.49}MnO_{2+y}$, and the formula for Zn-B as $Zn_x(OH)_jNa_zMnO_{2+y}$ on the basis of the assumption that all inserted anions are OH^-. The x, j, and z values in the Zn-B formula can be calculated from the chemical composition and charge balance relation:

$$2x + z - j = 0.49$$

where $x = 0.24$ and $z = 0.13$. Therefore, the j value of the OH^- content is 0.12, suggesting half of the Zn in Zn-B exists in the form of $Zn(OH)^+$ and the rest in Zn^{2+} form.

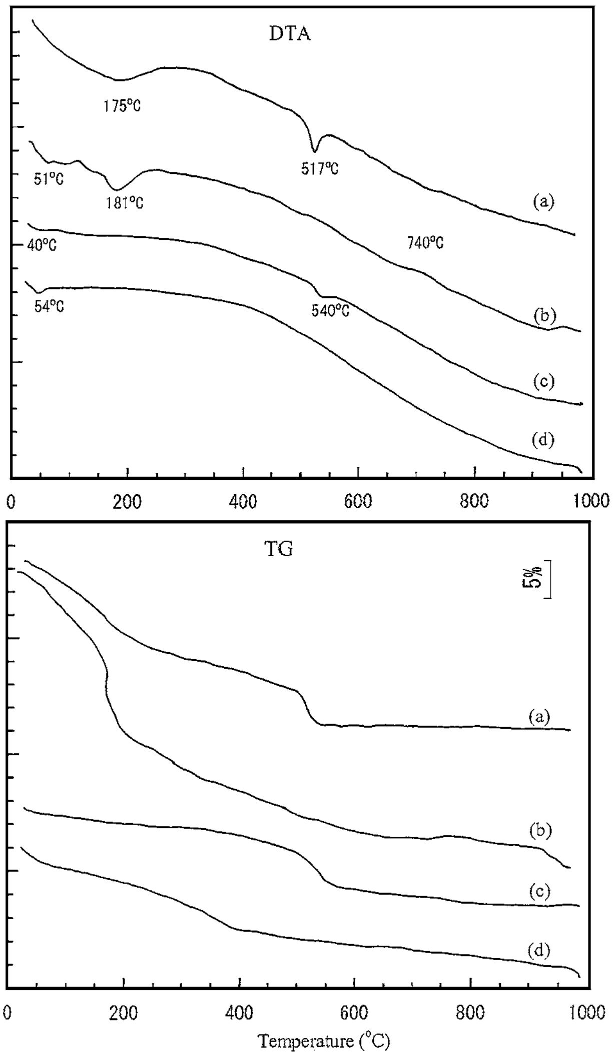

Figure 2 TG-DTA curves of (a) Zn-B, (b) Li-B, (c) ZB-300, and (d) lithiated ZB-300.

3.2. Thermal stabilities of Zn-birnessite and Li-birnessite

The thermal stabilities of Zn-B and Li-B were investigated by DTA–TG and XRD. Zn-B showed endothermic peaks around 175°C and 517°C, each corresponding to a weight loss (Fig. 2a). The broad endothermic peak around 175°C can be assigned to evaporation of surface adsorbed water and the dehydration of crystal water from the interlayer space. X-ray diffraction analysis (Fig. 3) indicates that the Zn-B retains its layered structure up to 300°C, even after losing the crystal water. The weight loss between 300 to 500°C can be assigned to the dehydration of OH groups in the interlayer space, accompanying destruction of the layered structure (Fig. 3). The endothermic peak around 517°C corresponds to the transformation of Zn-B to a $ZnMn_2O_4$ spinel phase, accompanying release of oxygen molecules. Li-B has endothermic peaks around 60 and 181°C, and corresponding weight losses (Fig. 2b), which is assigned to evaporation of surface adsorbed water and dehydration of crystal water from the interlayer space, respectively. The basal spacing of Li-B collapsed after dehydration of crystal water, and transformed to a spinel phase over 300°C (Fig. 4). The thermal behavior of Zn-B and Li-B is different to that of the Na-B precursor, which is stable up to 400°C, but transforms to a $Na_{0.4}MnO_2$ phase with a (2×3) tunnel structure and γ -Mn_2O_3 phase with heating to 500°C [18]. Our results indicate Zn-B is more stable than Li-B, due to the pillar effect of the Zn species in the interlayer space.

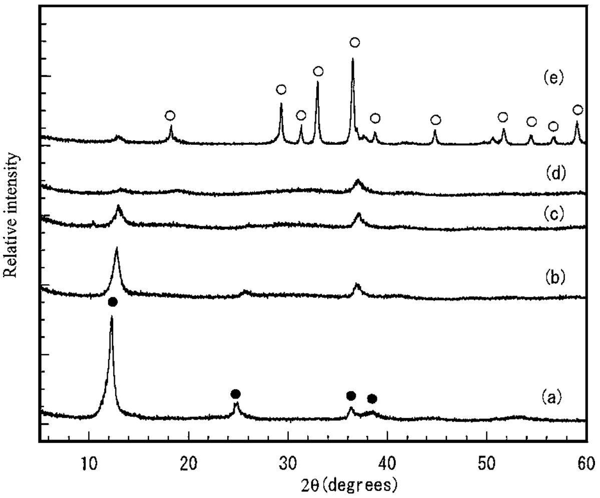

Figure 3 XRD patterns of (a) Zn-B and heated samples at (b) 200°C, (c) 300°C, (d) 400°C and (e) 500°C. ●: Birnessite phase,○: ZnMn$_2$O$_4$ spinel phase.

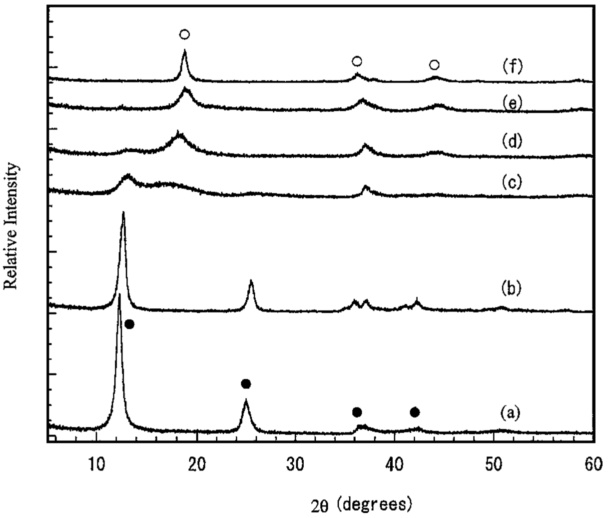

Figure 4 XRD patterns of (a) Li-B and heated samples at (b) 100°C, (c) 200°C, (d) 300°C, (e) 400°C and (f) 500°C. ●: Birnessite phase,○: Li-Mn-O spinel phase.

3.3. Lithiation reactions of Zn- and Li-birnessites in non-aqueous solution

The lithiation reaction in the LiI-actonitrile solution was carried out on Zn-B and Li-B. Prior to the lithiation reaction, Zn-B was pre-heated at 300 and 400°C to dehydrate crystal water in the interlayer space (the samples are designated ZB-300 and ZB-400, respectively). Four LiI-acetonitrile solutions, with LiI concentrations of 0.6, 1.2, 1.8, and 2.4 M, were used in the lithiation reaction, with Li/Mn molar ratios in the reaction system corresponding to 0.5, 1.0, 1.5, and 2.0, respectively. The reaction conditions and corresponding chemical compositions of the lithiated samples are summarized in Table II. The lithium content (Li/Mn molar ratio) in the lithiated samples is increased with increasing LiI concentration, up to 1.8 M, for both ZB-300 and ZB-400 samples, and is almost constant at greater concentrations. The lithium contents were much greater in lithiated ZB-300 samples than in lithiated ZB-400 samples, which suggest Li$^+$ is more easily inserted into the ZB-300 layered structure than into ZB-400 (in which the layered structure is partially destroyed; Fig. 3). Our XRD analysis (Fig. 5) reveals there are no structural changes in ZB-300 or ZB-400 samples after lithiation reaction, which indicates lithium insertion progresses by a topotactic reaction mechanism.

TABLE II Reaction conditions and chemical compositions of lithiated Zn- and Li-birnessites at 80°C for 60 hr

Sample	Concentration of LiI solution (M)	Composition (molar ratio) Zn/Mn	Li/Mn	Na/Mn	Z_{Mn}
ZB-300 (Zn-birnessite pre-heated at 300°C)					
	0.6	0.16	0.31	0.09	–
	1.2	0.14	0.42	0.09	–
	1.8	0.13	0.49	0.08	3.4
	2.4	0.17	0.45	0.10	–
ZB-400 (Zn-birnessite pre-heated at 400°C)					
	0.6	0.02	0.11	0.09	–
	1.2	0.01	0.16	0.09	–
	1.8	0.01	0.20	0.08	–
LB-100 (Li-birnessite pre-heated at 100°C)					
	1.8	–	1.08	–	3.9

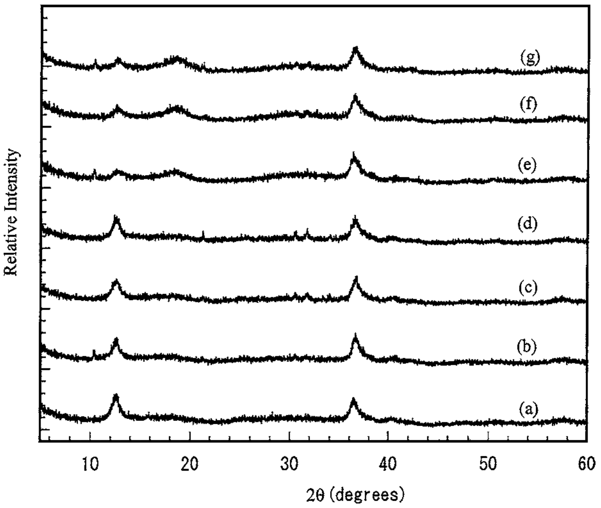

Figure 5 XRD patterns of lithiated (a–d) ZB-300 and (e–g) ZB-400 in (a, e) 0.6 M, (b, f) 1.2 M, (c, g) 1.8 M, and (d) 2.4 M LiI solutions at 80°C for 60 hr.

A similar lithiation reaction was also undertaken on Li-B that was pre-heated to 100°C (designated as LB-100). A sample with Li/Mn molar ratio of 1.08 was obtained after reaction of LB-100 with 1.8 M LiI solution at 80°C for 60 hr. The amount of inserted lithium (Li/Mn molar ratio = 0.61) by lithiation reaction was greater than in ZB-300 (Li/Mn molar ratio = 0.49) prepared under same reaction conditions (Table II). However, the layered structure of LB-100 partially changed after lithiation. Our results reveal that Zn-birnessite is more stable than Li-birnessite in the lithium insertion reaction. Chemical analysis indicates that the Z_{Mn} values for both Zn-B and Li-B decrease after the lithiation reaction (Table II), suggesting that the lithiation is a redox reaction, where Mn(IV) is reduced to Mn(III) accompanying the Li$^+$ insertion.

The effects of reaction temperature and reaction time were investigated for lithiation of ZB-300. The chemical compositions of lithiated samples after various

TABLE III Reaction conditions and chemical compositions of lithiated ZB-300 in 1.8 M LiI solution under different reaction time and reaction temperature conditions

Reaction condition		Composition (molar ratio)		
Time	Temperature	Zn/Mn	Li/Mn	Na/Mn
8 hr	80°C	0.17	0.43	0.13
1 day	80°C	0.18	0.51	0.16
3 days	80°C	0.18	0.49	0.11
7 days	80°C	0.07	0.46	0.17
3 days	25°C	0.19	0.33	0.08
3 days	100°C	0.20	0.56	0.10

reaction times and temperature conditions are summarized in Table III. The lithium content (Li/Mn molar ratio) is increased to 0.51 after a reaction time of 1 day, but is nearly constant after more than 1 day, at 80°C. An XRD study indicates no structural change in ZB-300 at these reaction conditions. The Li/Mn molar ratio in the sample is increased with increasing reaction temperature. A sample with Li/Mn molar ratio of 0.56 was obtained at 100°C, but the layer phase was partially transformed to a spinel phase after lithiation reaction.

3.4. Thermal stabilities of lithiated Zn- and Li-birnessite

The thermal stabilities of the lithiated ZB-300 and lithiated LB-100 were investigated by XRD and TG-DTA analyses. The TG-DTA analysis indicates a weight loss at around 300°C in the lithiated ZB-300 sample (Fig. 2d). The weight loss accompanies a structural change from a layered to spinel structure (Fig. 6). The layered structure of the lithiated ZB-300 was stable up to 200°C, and transformed completely to spinel at >500°C. The lithiated LB-100 completely lost its layered structure, and transformed to a spinel phase at 200°C (Fig. 7). These results indicate that lithiated Zn-birnessite has higher thermal stability than lithiated Li-birnessite, due to the pillar effect of Zn in the interlayer space of the birnessite.

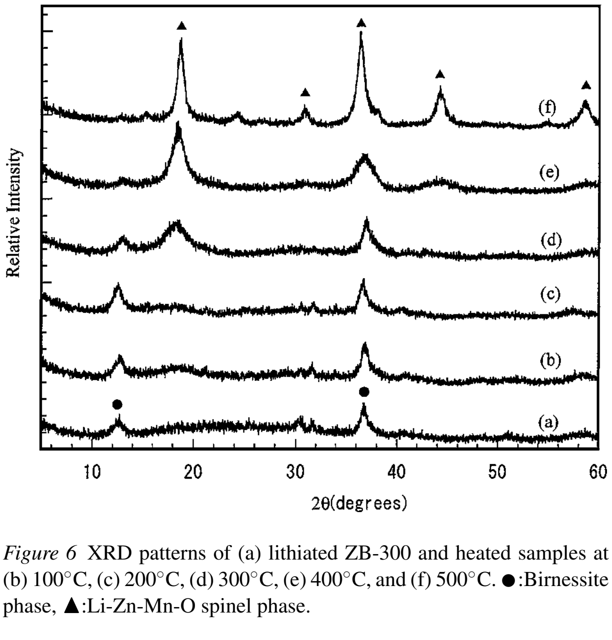

Figure 6 XRD patterns of (a) lithiated ZB-300 and heated samples at (b) 100°C, (c) 200°C, (d) 300°C, (e) 400°C, and (f) 500°C. ●:Birnessite phase, ▲:Li-Zn-Mn-O spinel phase.

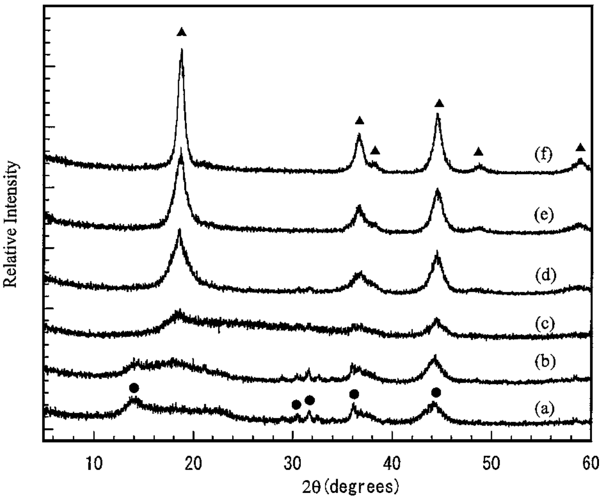

Figure 7 XRD patterns of (a) lithiated LB-100 and heated samples at (b) 100°C, (c) 200°C, (d) 300°C, (e) 400°C, and (f) 500°C. ●:Birnessite phase, ▲:Li-Mn-O spinel phase.

4. Conclusions

The Zn-birnessite can be synthesized by ion-exchange treatment of Na-birnessite with $ZnCl_2$ solution. In the ion-exchange reaction, Na^+ in the layered structure is exchanged with $Zn^{2+}$and $Zn(OH)^+$ complex ions. The Zn-birnessite shows higher stability than Li-birnessite. The Zn-birnessite can be lithiated by reaction with LiI-acetonitrile solution, and the lithiation progresses by redox topotactic reaction. The Zn species in the interlayer space act as a pillar for the stabilization of the layered structure in the lithiation reaction.

References

1. R. KOKSBANG, J. BARKER, H. SHI and M. Y. SAIDI, *Solid State Ionics* **84** (1996) 1.
2. J. KIM and A. MANTHIRAM, *Nature* **390** (1997) 265.
3. A. R. ARMSTRONG and P. G. BRUCE, *ibid.* **381** (1996) 499.
4. T. OHZUKU *et al.*, *Chemistry Express* **5** (1990) 733.
5. I. KOETSCHAU, M. N. RICHARD and J. R. DAHN, *J. Electrochem. Soc.* **142** (1995) 2906.
6. J. N. REIMERS, E. W. FULLER, E. ROSSEN and J. R. DAHN, *ibid.* **140** (1993) 3396.
7. R. J. GUMMOW, D. C. LILES and M. M. THACKERAY, *Mater. Res. Bull.* **28** (1993) 1249.
8. R. G. BURNS and V. M. BURNS, "Manganese Dioxide Symposium," Vol. 2 (I. C. MnO_2 Sample Office, Cleveland, OH, 1980) p. 97.
9. Q. FENG, H. KANOH and K. OOI, *J. Mater. Chem.* **9** (1999) 319.
10. P. STROBEL and C. MOUGET, *Mater. Res. Bull* **28** (1993) 93.
11. S. BACH, J. P. PEREIRA-RAMOS, N. BAFFIER and R. MESSINA, *Electrochimica Acta.* **36** (1991) 1595.
12. P. L. GOFF, N. BAFFIER, S. BACH and J. P. PEREIRA-RAMOS, *J. Mater. Chem.* **4** (1994) 133.
13. P. STROBEL, in MRS Symp. Proc. 1993, p. 63.
14. S. H. KIM, S. J. KIM and S. M. OH, *Chem. Mater.* **11** (1999) 557.
15. B. J. ARONSON, A. K. KINSER, S. PASSERINI, W. H. SMYRL and A. STEIN, *ibid.* **11** (1999) 949.

16. P. LE. GOFF, N. BAFFIER, S. BACH and J. P. PEREIRA-RAMOS, *Mater. Res. Bull.* **31** (1996) 63.
17. Q. FENG, L. LIU and K. YANAGISAWA, *J. Mater. Sci. Lett.* **19** (2000) 1567.
18. L. LIU, Q. FENG and K. YANAGISAWA, *ibid.* **19** (2000) 2047.
19. Q. FENG, H. KANOH, Y. MIYAI and K. OOI, *Chem. Mater.* **7** (1995) 1226.
20. P. STROBEL, F. L. CRAS, S. ROHS and L. PONTONNIER, *Mater. Res. Bull.* **31** (1996) 1417.
21. Y. XU, Q. FENG, K. KAJIYOSHI and K. YANAGISAWA, *Chem. Mater.*, in press.

Received 1 May
and accepted 29 November 2001